Biomedical Microdevices 5:2, 157–162, 2003

Nanotechnology:

Section Editors Dr Steve Lee and Dr Nicanor Moldovan

DNA Assembly on 2-Dimensional Array of Colloidal Gold

*Cunwang Ge,[1] Jianhui Liao,[1] Yihong Wang,[1] Kunji Chen,[2] and Ning Gu[1]**

[1]National Laboratory of Molecular and Biomolecular Electronics, Southeast University, Nanjing, 210096, P.R. China
E-mail: guning@seu.edu.cn
[2]State Laboratory of Solid-state Microstructure, Nanjing University, Nanjing 210093, P.R.China

Abstract. **The primary object of this contribution is to self-assemble DNA on 2-dimensional array of 1-dodecanethiol-encapsulated colloidal gold (2-DACG). The 2-DACG film was deposited by Langmuir-Blodgett (LB) technique. Through phase transfer of aqueous colloidal gold particles into ethanol solutions containing 1-dodecanethiol, the hydrophobic gold colloidal nanoparticles were accomplished. In the presence of traces of 1-dodecanethiol, the gold nanoparticels were transferred via LB technique to a freshly cleaned gold electrode and 2-DACG of close-packed, ordered monolayer was obtained. The 2-DACG was then used as a substrate for the immobilization of DNA under a controled potential of + 0.20 V vs. saturated calomel electrode (SCE). The properties of 2-DACG before and after the DNA assembly were investigated by means of transmission electron microscopy (TEM), atomic force microscopy (AFM), cyclic voltammetry (CV) and electrochemical impedance spectroscopy (EIS). The results indicated that 2-DACG deposited by LB technique was suitable as a substrate for DNA self-assembly.**

Key Words. **DNA assembly, 2-dimensional array, thiol encapsulated colloidal gold, substrate**

1. Introduction

DNA has long been pursued as the structural basis for the supramolecular ''bottom-up'' engineering of electrical nanocircuits (Yan et al., 2002). DNA has a special double-helix structure with 1-dimensional charge transport, phosphorus bridges and hydrogen bonds, which may be suitable for tunnel junction and capacitance (Porath et al., 2000; Ben-Jacob et al., 1999). The use of DNA for the selective positioning of macromolecular components, production of nanostructured DNA scaffolds, as well as the DNA-templated synthesis of nanometer-sized and mesoscopic complexes, are very active subjects of current research communities. The construction of DNA-based electronic nanodevices is possible and will also be a predominant technique of new integrated circuit probes with important benefits of miniaturization, low power requirements, high efficiency and low heat generation. DNA self-assembly has been considered as a fundamental methodology for the realization of molecular logic circuits, as well as a crucial step in the construction of DNA-based nanodevices (Niemeyer, 1999).

Based on the self-assembled monolayer (SAM) technique, a number of different methods for immobilizing DNA onto electrodes have been recently reported. Physical adsorption was accomplished by Pang and Abruña (2000) with microsamples. Controlled electrostatic adsorption was adopted to anchor DNA to carbon paste (Wang et al., 1996) and HOPG electrodes (Wu et al., 2000). Herne et al. (1997) and Levicky et al. (1998) synthesized mercapto-oligonucleotides, which were directly immobilized on a gold electrode. DNA has also been covalently immobilized onto some modified electrodes using the activation-coupling reagent (Zhao et al., 1999) or streptavidin/avidin conjugates (Niemeyer et al., 1998). We have recently developed a new approach based on the potential control to handle DNA self-assembly covalently onto a self-assembly monolayer (Ge et al., 2002). In general, physical adsorption of DNA onto the bare electrode is simple, but neither carbon paste nor HOPG electrodes are suitable for the DNA-based device. Preparation of functional mercaptocontaining DNA is very labor-intensive, and the procedure for the modification of DNA is rather complicated and unreliable. Covalent immobilization of DNA onto gold via SAM is practicable for DNA-based biosensors, the efficiency of immobilization, however, is not very good because of the multi-step sequence. The approach present here is to simplify the procedure of DNA self-assembly with sufficient affinity on the basis of potential control.

*Corresponding author.

Colloidal gold has been used to enhance the DNA immobilization on the electrode (Cai et al., 2001) and to reinforce DNA colorimetrical detection (Taton et al., 2000). In particular, the Coulomb blockade (Huang et al., 2000), the most significant phenomenon of single-electron tunneling, has been observed in nanostructures made from alkanethiol-encapsulated gold nanoparticles at room temperature. Taking a cue from Huang et al. (1998) for preparation of 2-DACG by phase transfer, our efforts are focused on assembly of calf thymus DNA under potential control onto the 2-DACG. The method is simple, convenient, reliable and applicable for DNA studies. The results prove that the 2-DACG satisfy DNA self-assembly, which could be further used to study the interaction of DNA with other molecules, and to establish DNA-based nanoelectronic devices.

2. Materials and Methods

2.1. Materials

Calf thymus DNA (Sino-American Biotechnical Co., China) was purified as previously described. 1-Dodecanethiol (Fluka) was used as received. $[Co(phen)_3](ClO_4)_3$ was prepared according to the literature (Dollimore et al., 1973). Flat gold foils for atomic force microscopic (AFM) experiments were prepared with template-stripped technique reported by Wagner et al. (1995) with minor modifications. All other chemicals used were of analytical purity. Millipore water was distilled twice, and sterilized in Milli-Q plus (Millipore Corp., Bedford, MA).

2.2. Apparatus

The isotherms of pressure-area per particle (π-A) were performed on an ALT KSV-5000 trough (KSV Instruments, Helsinki, Finland) equipped with a Wilhelmy plate as a surface pressure sensor. Transmission electron microscopic (TEM) measurements were carried out using a JEM-200CX transmission electron microscope at 120 KV (JEOL Co., JP). AFM images were collected with a Nanoscope IIIa AFM (American Digital Instruments, Santa Barbara, CA) with a tip of silicon nitride in tapping mode at room temperature in air. The electrochemical measurements were performed on a CHI 660A workstation (CH Instrument Co., Austin, TX) as our previous report (Ge et al., 2002). The electrochemical cell consisted of a three-electrode system with gold or modified gold electrode (2 mm in diameter) as the working electrode, a saturated calomel electrode (SCE) and a platinum wire as the reference and the counter electrode, respectively. The experimental temperature was controlled at $25 \pm 1\,^{\circ}C$. AC impedance experiments were carried out within the frequency range of 10 mHz to 100 kHz. A 10 mV RMS sinusoidal potential signal was applied to the electrode held at open circuit potential.

2.3. Fabrication of 2-DACG

The fabrication process consisted of two main steps: (1) Preparation of 1-dodecanethiol-encapsulated gold particles from colloidal gold particles. The colloidal gold particles of ~ 11 nm in diameter were synthesized by an established procedure using a reduction of chloroauric acid ($HAuCl_4$) with trisodium citrate and tannic acid (Slot and Geuze, 1985). Hydrophobic gold nanoparticles were synthesized through phase transfer of aqueous colloidal gold particles into ethanol solutions containing 1-dodecanethiol and followed by removing any unreacted 1-dodecanethiol (Huang et al., 2000). As a result, a well-defined monolayer of 1-dodecanethiol is expected to be generated on the surface of each gold nanoparticle. (2) Self-organization of an ordered close-packed array of gold nanoparticles encapsulated by 1-dodecanethiol on a hydrophobic substrate. 2-DACG was obtained by spreading 350 μL chloroform solution containing 0.1 mg/mL 1-dodecanethiol-capped colloidal gold and 0.04 mM 1-dodecanethiol onto pure water. As will be discussed later, the addition of 1-dodecanethiol into the chloroform solution was to make a hydrophobic gold electrode surface so as to improve the quality of the LB film formed. After 15 minutes evaporation, the monolayer was compressed at a typical rate of 5 mm/min. Isotherms of surface press versus mean molecular area (π-A) were measured at $17 \pm 0.2\,^{\circ}C$. After stabilization of the 2-DACG monolayer and measurement of the π-A isotherms, the monolayer was transferred to the substrate by retracting a carbon-coated copper TEM grid, or to a gold electrode, by vertical dipping at a surface pressure of 13 mN/m and a dipping speed of 1.0 mm/min. The substrate surface was set to be parallel to the moving direction of the barrier.

2.4. DNA assembly at Langmuir-Blodgett films on the gold electrode

A 2.0 mm in diameter gold electrode (CH Instrument Co Austin, TX) was used throughout the electrochemical measurement. Before use, the electrode was polished with a w5 abrasive paper, subsequently with 0.25 and 0.05 μm alumina slurries (Buehler Ltd., Lake Bluff, IL), followed by ultrasonification in ethanol and water for 2 minutes respectively. In addition, prior to retracting of Langmuir-Blodgett films, the pretreated electrode was also treated with the ''piranha solution'' (concentrated $H_2SO_4/30\%H_2O_2$, 7:3 in v/v) for 5 minutes at room temperature and subsequently rinsed thoroughly with twice distilled water and finally ultrasonically cleaned with ethanol and twice distilled water for 3 minutes, respectively. The electrode then was retracted with a

Langmuir-Blodgett film of 2-DACG and dried by an infrared lamp so that a layer of close-packed nanogold clusters was deposited on the surface of the gold electrode (denoted as LBAu/Au). The electrode was subsequently used as the working electrode under a controled potential of + 0.2 V vs. SCE for 1 hour in 1 mg/mL calf thymus DNA solution consisting of 5 mM NaCl and 5 mM Tris-HCl buffer with pH = 7.1. Before the immobilization the DNA solution had been incubated at 37 °C for 30 minutes to extend coil state. The DNA modified electrode (denoted as DNA/LB Au/Au) was then soaked in Tris-HCl buffer for 10 minutes to remove any non-specifically adsorbed DNA.

2.5. Nonlinear simulation of equivalent circuits

Electrochemical impedance spectroscopic data of the self-assembly monolayer system were collected on a CHI workstation, and modeled using the Randles equivalent circuit with the circuit description code of R(C[RW]) (Bard and Faulkner, 2001). Capacitances of the double-electron layer were simulated by nonlinear least squares using the EQUIVCRT.PAS (V 4.51) program written by Boukamp (1993).

All experiments were conducted at a room temperature of ~20°C, unless otherwise stated.

3. Results and Discussion

3.1. The mechanism of DNA assembly on LB monolayer

A hydrophilic surface is expected to be formed after the gold electrode freshly cleaned by the procedure described in Section 2.4. Clearly, an electrode with this kind of hydrophilic surface is not a suitable substrate for 2-DACG, since the surface property of the nanoparticles is hydrophobic. To get rid of this kind of problem, traces of 1-dodecanethiol (40 μM) were added to the LB trough with a chloroform solution containing 0.1 mg/mL 1-dodecanethiol-capped colloidal gold. When a clean gold electrode was dipped into and touched with the gold nanoparticle LB monolayer containing traces of free 1-dodecanethiol species, the electrode could immediately react with the thiol and form a self-assembled thiol monalayer that possesses hydrophobic properties and is suitable for the retracting of LB monolayer of 2-DACG.

There are various interactions between DNA and any other molecules, such as electrostatic interaction, hydrophobic interaction and intercalation (Pasternack and Gibbs, 1983). Many hydrophobic groups exist inside the bases of DNA, which could protect Watson-Crick hydrogen bonding of base pairs against water. When a drop of calf thymus DNA solution was cast onto the 2-DACG monolayer, water was evaporated from DNA with the fervour of enthalpy. The DNA was contracted and the hydrophobic dodecyl group could be inserted into the groove of DNA through the hydrophobic interaction. The hydrophobic interaction is caused by the withdrawal of hydrophobic substances from the aqueous solution (Israelachvili, 1995). The affinity between DNA and 2-DACG was stronger than that of bare gold and DNA, which was tested by our preliminary experiment. When a 2-DACG of gold electrode modified with DNA was stored in 50 mM NaCl and 5 mM Tris-HCl buffer with pH = 7.1 for 2 days at 4 °C, the electrode still retained more than 90% of its initial response to electro-active species. The flexibilities of the hydrophobic group of 1-dodecanethiol outside the encapsulated colloidal gold could play an important role, since this kind of group could be freely inserted into the strands of DNA. In contrast, a bare gold electrode with a rigid surface could not be readily assembled with the rigid skeleton of DNA, and in this case low affinity between the bare gold and the DNA is not unexpected. Additionally, the hydrophobic interaction might also promote assembly of the alkyl chain to DNA, although the weak physical adsorption and other interaction cannot be entirely excluded (Lipkowski, 1999).

3.2. Formation of close-packed 2-DACG

Figure 1 shows the surface pressure versus area per cluster for 11 (± 2.0) nm in diameter 1-dodecanethiol-encapsulated colloidal gold. In the region of the area per cluster of about 600 to 280 nm^2, the surface pressure is very small because of the large distance between particles. Then, from about 280 to 130 nm^2 area per cluster, a gradual increase in surface pressure is observed, which could be attributed to the dodecyl constriction of the colloidal gold clusters. From the point of about 130 nm^2 area per cluster, the surface pressure increases rapidly, indicating that an ordered close-packed

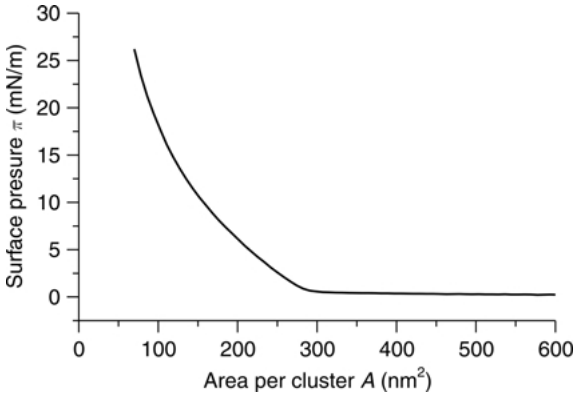

Fig. 1. *Surface pressure vs. area per particle (π – A) isotherms for 1-dodecanethiol-encapsulated colloidal gold measured at ~17°C.*

monolayer of 2-DACG starts to form. We found that a surface pressure of 13 mN/m, which corresponds to about 132 nm^2 area per cluster, is optimal for an ideal monolayer formation. Such a condition was applied to fabricate the monolayer on both TEM grids and gold electrodes reported in this paper.

Figure 2 shows the TEM micrograph of a close-packed 2-DGC monolayer. Clearly, a hexagonal close-packed monolayer structure is obtained. The electron diffraction pattern revealed that the 2-DACG had a face-centerd-cubic (FCC) structure with a cell parameter of $a = 4.079 \pm 0.015$ Å in the image distance of 137 cm with the diffraction character of two close and one thin (not shown). The estimated area per 1-dodecanethiol-encapsulated gold particle, with a diameter of 11 nm, is about 95 nm^2. Thus, under a surface pressure of 13 mN/m, the particle coverage is about 72%. The unoccupied area may be assigned to the arrangement defects of the FCC structure, the disparity of the gold particles as well as the free thiol molecules present in the system. Compared the gold films obtained by vacuum evaporation (Ge et al., 2002), we found that the pattern quality of the 2-DACG obtained on a TEM copper grid coated with carbon was even better. Since both the surfaces for the carbon-coated copper grid and for the thiol modified gold electrode are hydrophobic, the property of the LB film observed on the TEM grid should be also operative for the gold electrode. Therefore, the LB film deposited on a gold electrode could be used as a good substrate for the assembly of DNA.

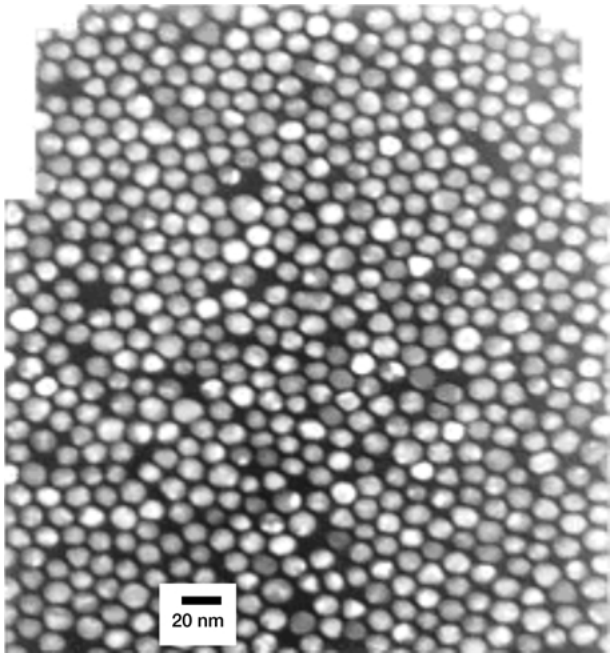

Fig. 2. *TEM micrographs of 2-DACG monolayer prepared by LB technique.*

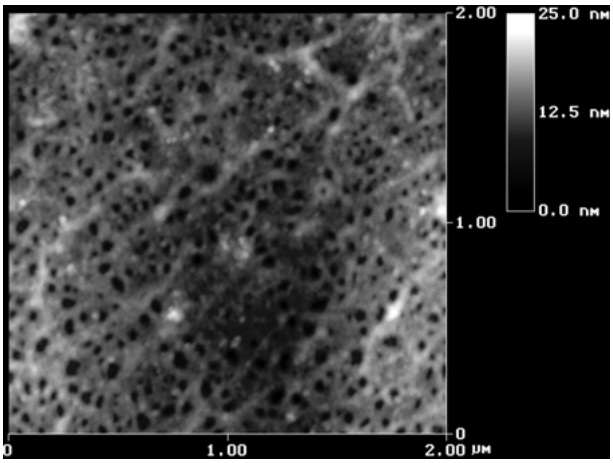

Fig. 3. *Tapping mode AFM images of DNA assembled 2-DAGC film deposited by Langmuir-Blodgett (LB) on a gold electrode at a controlled potential of + 0.2 V vs SCE.*

3.3. Patterns of DNA on 2-DACG

The patterns of DNA assembled on 2-DACG at + 0.2 V vs. SCE were directly visualized using AFM. As shown in Figure 3, the meshy pattern of winding DNA was clearly discernable with the displays of the individual widths of 15 ~ 20 nm to some extent of aggregation. The individual colloidal gold nanoparticles could not be resolved because of the effects of AFM magnification as well as the possible interactions between the tip and the DNA sample (Hansma et al., 1992; Lyubchenko et al., 1993). These kinds of interactions include capillary adsorptions and electrostatic force effects.

3.4. Cyclic voltammetric characterization of different electrodes

To preserve DNA physiological pH and to avoid DNA-strand splitting effects (Carter et al., 1989), a pH 7.1 solution with a constant ionic strength of 50 mM NaCl and 5 mM Tris-HCl buffer was used during CV experiments. The properties of differently modified electrodes were examined by CV using 0.12 mM $[Co(phen)_3](ClO_4)_3$ as an electroactive reagent that was added in the Tris-HCl buffer solution. Figure 4 shows the CV curves obtained at a scan rate of 100 mV/s for bare Au (curve 1), LBAu/Au (curve 2) and DNA/LBAu/Au (curve 3). Comprehensively, the following features were observed:

(1) The redox peak currents of $Co(phen)_3^{3+}$ species at the DNA/LBAu/Au electrode were much larger compared with those at LBAu/Au and bare Au electrodes, while significantly less peak currents were observed at the LBAu/Au electrode with

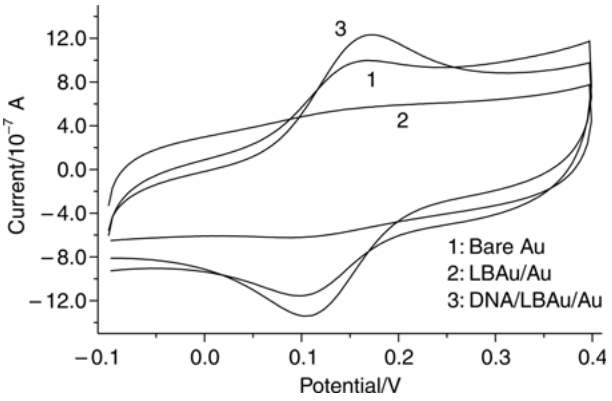

Fig. 4. *Cyclic voltammograms obtained for differently modified electrodes at a scan rate of 100 mV/s in pH 7.1 Tris–HCl buffer solution containing 0.12 mM [Co (phen)$_3$](ClO$_4$)$_3$.*

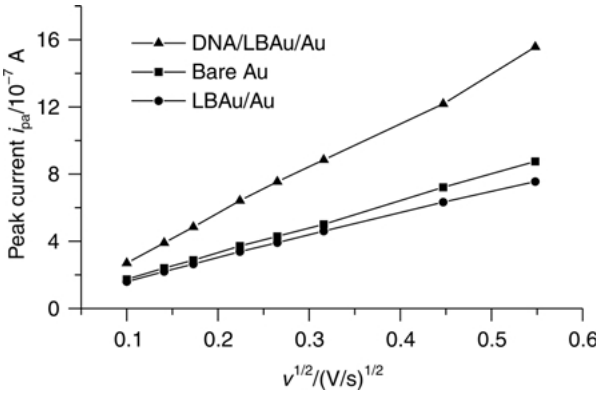

Fig. 5. *Comparison of oxidation peak currents vs $v^{1/2}$ for bare Au, LBAu/Au, and DNA/LBAu/Au electrodes in pH 7.1 Tris-HCl buffer solution containing 0.12 mM[Co(phen)$_3$](ClO$_4$)$_3$.*

respect to those obtained at the bare Au electrode. These data suggest that a good quality of 2-DACG was formed on the surface of the gold electrode via LB technique, and that the electroactive species can be weakly adsorbed on and/or intercalated into the DNA immobilized on the LBAu/Au electrode.

(2) At the DNA/LBAu/Au electrode, the ratio of the oxidation peak current, i_{pa}, to the reduction peak current, i_{pc}, was found to be greater than 1, and the ratio increased with the scan rate used accompanying the reduction peak potential slightly shifted positively. This suggests that the electroactive species adsorption/intercalation processes occurred at the DNA electrode, and that the reduced form of the electroactive species can be bound to the electrode relatively stronger compared to its original state. Similar behavior has been also reported previously (Carter et al., 1989).

(3) In the case of the bare gold electrode, the peak potential separation ($\Delta E_p = E_{pa} - E_{pc}$) and the peak shape $|E_{pc} - E_{p/2}|$, were found to be between 60–70 mV, independent of potential sweep rate ($10 \leq v \leq 100\,\mathrm{mV/s}$), indicating that the reduction of $[\mathrm{Co(phen)_3}]^{3+}$ at the electrode is an one electron transfer reversible process. A linear correlation between the oxidation peak current and the square root of the scan rate $v^{1/2}$ was observed (Figure 5), as expected for a diffusion controled electrochemical process. For all electrodes, $R \geq 0.999$ and $P \leq 0.001$, respectively (from the linear fitting in Figure 5). On the other hand, at the DNA/LBAu/Au electrode, the oxidation peak current increases rapidly with the $v^{1/2}$, which is consistent with the electroactive species adsorption/intercalation behavior occurred at the surface of the electrode.

3.5. AC impedance analysis for different electrodes

AC impedance data for bare Au, LBAu/Au and DNA/LBAu/Au electrodes were recorded in the electrolyte solution of 1 mM $K_3Fe(CN)_6$ and 1 mM $K_4Fe(CN)_6$ containing 0.1 M KCl, and are presented in Figure 6. Z' and Z'' represent for the real part and the imagine part of impedance, respectively. As would be expected, with the formation of the LB film on the surface of the bare gold electrode, the charge transfer resistance (R_c) significantly increased, indicating a high coverage of the LB film on the bare gold electrode had been achieved. Similarly, after immobilization of DNA onto the LBAu/Au electrode $[R_c^{\mathrm{LBAu/Au}} \sim (4.1 \pm 0.6) \times 10^2\,\mathrm{ohm}]$, a further increase in charge transfer resistance obtained $[R_c^{\mathrm{DNA/LBAu/Au}} \sim (1.1 \pm 0.1) \times 10^3\,\mathrm{ohm}]$. The above data is also consistent with the electrode capacitance changes. After assembly of DNA onto the LBAu/Au electrode, the capacitance changed from $(9.3 \pm 0.4) \times 10^{-7}\,\mathrm{F}$ for LBAu/Au to a small value of $(7.1 \pm 0.4) \times 10^{-7}\,\mathrm{F}$, since the DNA layer formed on the LBAu/Au electrode

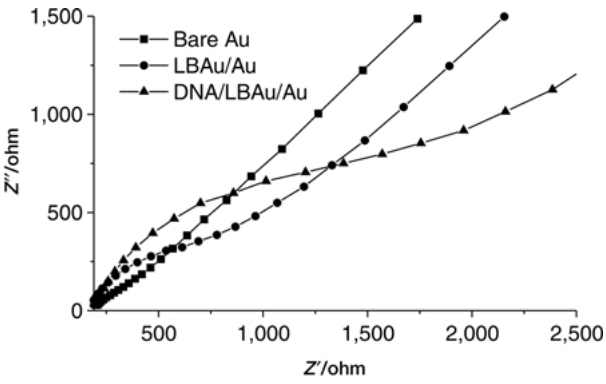

Fig. 6. *EIS plots for bare Au, LBAu/Au and DNA/LBAu/Au electrodes measured in 1 mM$K_3Fe(CN)_6$/1 mM$K_4Fe(CN)_6$ containing 0.1 M KCl.*

could be treated as a capacitor in series to the LB film. Thus, as shown previously in Section 3.4, a stable 2-DACG layer can be formed on a bare gold electrode, which can then be used as a substrate for the immobilization of DNA assembly.

4. Conclusion

This work demonstrates that 2-DACG can be used as a substrate for DNA self-assembly. Due to the simplicity, flexibility, and practicality of this method, its wide applications in the development of future nanoelectronic devices and electrochemistry studies would be expected. The technique reported in this paper is also of great significance for the control of DNA self-assembly, and which may be very useful in the field of DNA-based devices studies, although further investigations are clearly required before any practical applications.

Acknowledgement

This work was supported by the National Natural Science Foundation of China (Grant No.60171005 and Grant No. 60121101), and the Natural Science Foundation of Jiangsu (China) (Grant No. BK2001131). The authors also wish to thank Dr. Wujian Miao (University of Texas at Austin) for the contribution.

References

A.J. Bard and L.R. Faulkner, *Electrochemical methods,* Chapter 10, 2nd edn (John Wiley & Sons, New York, 2001).

E. Ben-Jacob, Z. Hermon, and S. Caspi, Physics Letters A **263**, 199 (1999).

B.A. Boukamp, *Equivalent Circuits. Users Manual,* 2nd edition (University of Twente, The Netherlands, 1993).

H. Cai, C. Xu, P.G. He and Y.Z. Fang. J. Electroanal. Chem. **510**, 78 (2001).

M.T. Carter, M. Rodriguez, and A.J. Bard, J. Am. Chem. Soc. **111**, 8901 (1989).

L.S. Dollimore and R.D. Gillard, J. Chem. Soc. Dalton Trans. 933 (1973).

C.W. Ge, Y.B. Tan, J.H. Liao, Y. Zhang, H.Q. Zhang and N. Gu, Chinese Science Bulletin **47**(5), 370 (2002).

H.G. Hansma, R.L. Sinsheimer, M.O. Li and P.K. Hansma, Nucleic Acids Research **20**(14), 3585 (1992).

T.M. Herne and M.J. Tarlov, J. Am. Chem. Soc. **119**, 8916 (1997).

S. Huang, G. Tsutsui, H. Sakaue, S. Shingubara, and T. Takahagi, J. Vac. Sci. Technol. B **18**, 2653 (2000).

S. Huang, H. Sakaue, S. Shingubara, and T. Takahagi, Jpn. J. Appl. Phys. **37**, 7198 (1998).

J.N. Israelachvili, *Intermolecular and Surface Forces* (Academic Press, London, 1995).

R. Levicky, T.M. Herne, M.J. Tarlov, K. Sushil, and S.K. Satija, J. Am. Chem. Soc. **120**(38), 9787 (1998).

J. Lipkowski, Can. J. Chem **77**, 1163 (1999).

Y. Lyubchenko, L. Shlyakhtenko, R. Harrington, P. Oden and S. Lindsay, Proc. Natl. Acad. Sic. USA **90**(6), 2137 (1993).

C.M. Niemeyer, Appl. Phys. A—Materials Science & Processing **68**, 119 (1999).

C.M. Niemeyer, W. Bürger, and J. Peplies, Angew. Chem. Int. Ed. **37**, 2265 (1998).

D.W. Pang and H.D. Abruña, Anal. Chem. **72**, 4700 (2000).

R.F. Pasternack and E.J. Gibbs, Biochemistry **22**, 5409 (1983).

D. Porath, A. Bezryadin, S. de Vries and C. Dekker, Nature **403**, 635 (2000).

J.W. Slot and H.J. Geuze, Eur. J. Cell Biol. **38**, 87 (1985).

T.A. Taton, C.A. Mirkin, R.L. Letsinger, Science **289**, 1757 (2000).

P. Wagner, M. Hegner, H.J. Güntherodt and G. Semenza, Langmuir **11**, 3867 (1995).

J. Wang, X. Cai, G. Rivas, and H. Shiraishi, Anal. Chim. Acta **326**, 141 (1996).

L. Wu, J. Zhou, J. Luo, and Z. Lin, Electrochimica Acta **45**, 2923 (2000).

H. Yan, X. Zhang, Z. Shen, and N.C. Seeman, Nature **415**, 62 (2002).

Y. Zhao, D. Pang, S. Hu, Z.L. Wang, J.K. Cheng and H.P. Dai, Talanta **49**, 751 (1999).